Journal of Solid State Chemistry **153,** 152–157 (2000)
doi:10.1006/jssc.2000.8766, available online at http://www.idealibrary.com on IDEAL®

Independent $\vec{q}$ and $2\vec{q}$ Distortions in the Incommensurately Modulated Low-Temperature Structure of $NiTa_2Se_7$

Jens Lüdecke, Martin Schneider, and Sander van Smaalen

Laboratory of Crystallography, University of Bayreuth, 95440 Bayreuth, Germany
E-mail: jens.luedecke@uni-bayreuth.de

Received January 4, 2000; in revised form May 3, 2000; accepted May 11, 2000; published online June 29, 2000

The modulated low-temperature structure of $NiTa_{1.98}Nb_{0.02}Se_7$ has been determined by X-ray diffraction using synchrotron radiation. The superspace group of the modulated structure at 15 K is $C2/m(0, q_b, 0)s0$ with $q_b = 0.483(2)$. The lattice parameters were determined to $a = 13.807(6)$ Å, $b = 3.483(1)$ Å, $c = 18.564(11)$ Å, and $\beta = 108.95(4)^\circ$ with $Z = 4$. Satellite reflections up to second order were measured. Refinement with first- and second-order harmonic components of the modulation functions converged to $R = 0.059$. The first-order harmonic was found predominantly on the double chain of Ni and Se2 atoms. Shifts were found parallel to the $\vec{a}$ and $\vec{c}$ axes, in good agreement with earlier investigations. The major part of the second harmonic was found on the Ta2 atoms, with amplitudes of secondary importance on the surrounding Se atoms. Shifts of the Ta2 atoms were found parallel to $\vec{b}$, thus forming a longitudinal wave. It is argued that the modulations according to the first-order and the second-order harmonics should be considered as independent CDW's. © 2000 Academic Press

Key Words: **incommensurate structures; charge density waves; phase transitions.**

1. INTRODUCTION

$NiTa_2Se_7$ belongs to the layered transition-metal chalcogenides of which several display interesting physical properties like charge-density-wave (CDW) states due to their quasi-low-dimensional properties (1). The structure of $NiTa_2Se_7$ is monoclinic. It consists of two inequivalent chains of Ta atoms along the monoclinic $\vec{b}$ axis. The atoms of one chain are in trigonal prismatic coordination by Se atoms, similar to the structure of $TaSe_3$. The atoms of the other chain are in octahedral coordination by Se atoms, similar to the structure of 1T-$TaSe_2$ (Fig. 1). The two types of chains are separated by chains of Ni atoms in highly distorted octahedral coordination (2). The strings of metal atoms support quasi-one-dimensional electron bands along the $\vec{b}$ axis.

A phase transition toward a CDW state has been observed at a temperature of 52.5 K (3). A CDW state is characterized by a modulation of the atomic positions combined with a modulation of the charge in a quasi-one-dimensional electron band. The modulation wave vector is determined as twice the Fermi wave vector (4). For $NiTa_2Se_7$ the CDW shows up in X-ray diffraction by weak satellite reflections characterized by the modulation wave vector $\vec{q} = (0, 0.483, 0)$ (3). Recently an analysis of the incommensurately modulated structure was performed using the intensities of first-order satellites (5). Major modulation amplitudes were found on the Se2 and Ni atoms including the surrounding atoms. The modulation was found to be parallel to the $\vec{a}$ and $\vec{c}$ axes and thus represents a transverse wave. This situation is different from what was observed for other CDW compounds [e.g., $NbSe_3$ (6)], for which a longitudinal modulation was found. The transverse character of the modulation can only be understood as a CDW, if one assumes that the observed variation of the bond valence of the bond between Ni and Se2 corresponds to the charge-density variation (5).

In order to obtain further insight into the nature of the CDW state, $NiTa_2Se_7$ crystals with various amounts of Nb doping were synthesized and their properties were characterized. The distribution of Nb over the two independent Ta sites was found to be uneven, and doping was found to suppress the transition temperature by about 10 K for each percent of Nb, as will be discussed in detail elsewhere (7). In the present paper, the results are reported of an X-ray diffraction study on the CDW state of the doped sample $NiTa_{1.98}Nb_{0.02}Se_7$. It is found that the modulation involves both the Ni–Se2 double chain and the chain of Ta2 atoms. The detailed modulated structure will be presented, and the implications for the understanding of the CDW state in $NiTa_2Se_7$ will be discussed.

2. EXPERIMENTAL PROCEDURES

$NiTa_{2-x}Nb_xSe_7$ samples with black metallic gloss and different concentrations x of niobium were prepared using the gas transport technique (2). From the batch with

0022-4596/00 $35.00

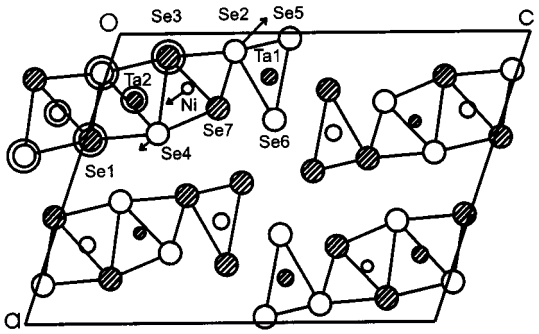

FIG. 1. Projection of the unit cell of $NiTa_2Se_7$ along $\vec{b}$. Open circles represent atomic positions at $y = 0.5$; hatched circles at $y = 0$. The modulations with the first-order harmonics on Ni, Se2, and Se4 are indicated by arrows; the modulations with the second-order harmonics on Ta2, Se1, and Se3 are indicated by an extra circle in the upper left asymmetric unit.

$x = 0.02$ a needle-shaped crystal with dimensions of $0.035 \times 0.05 \times 4$ mm was chosen for X-ray diffraction experiments on beamline D3 at Hasylab (DESY, Hamburg). Unfortunately, it was not possible to find a crystal of good quality and sufficient scattering volume whose length did not exceed the diameter of the beam. Cutting the crystals was not possible without causing severe damage to the sample. Therefore, a long needle-shaped sample was selected for the diffraction experiment.

The crystal was mounted on a closed-cycle helium cryostat on a Huber four-circle diffractometer. Diffraction experiments were performed at a temperature of 15 K using a wavelength of $\lambda = 0.5608$ Å. The lattice parameters were determined from the setting angles of 12 orientation reflections in the range $12^\circ < \theta < 14^\circ$ as $a = 13.807(6)$ Å, $b = 3.482(1)$ Å, $c = 18.564(11)$ Å, and a monoclinic angle of $\beta = 108.95(4)^\circ$.

Sharp reflections were observed at the expected positions for the main reflections ($m = 0$) and for the first- and second-order satellite reflections ($|m| = 1, 2$), according to an indexing of the diffraction pattern with four integers ($hklm$).

$$\vec{S} = h\vec{a}^* + k\vec{b}^* + l\vec{c}^* + m\vec{q}. \qquad [1]$$

The three components of the modulation wave vector $\vec{q}$ were confirmed to be $(0, 0.483(2), 0)$ using q scans along the three directions of reciprocal space. Intensities of the main Bragg reflections and satellites up to second order were collected by ω scans in the range $10^\circ < \theta < 18^\circ$ which already covers a fair amount of reciprocal space due to the short wavelength used ($0.31 < \sin(\theta)/\lambda < 0.55$). For θ values below 10°, background radiation from the Be shields of the closed-cycle cryostat was too high to measure the weak satellite reflections, so this region was excluded from the measurement. For the same reason, data collection could not be performed with an area detector because the high background cannot be eliminated any more by a detector collimator, as it was done in the present experiment using a point detector. In total the intensities of 2360 reflections with $-14 < h < 14$, $-4 < k < -1$, and $-18 < l < 18$ were measured. The variations in scattering volume due to length of the sample exceeding the diameter of the beam were minimised by choosing an optimal ψ value for the data collection. As discussed in Section 3, these variations affect only the values of the temperature factors, but they did not hamper the accurate determination of the structural and modulation parameters.

The FWHM of the main reflections was less than 0.1°. Due to the small angular divergence of the incident beam, this width represents the mosaic spread of the sample. Intensities were corrected for the variations of the intensity of the incoming synchrotron radiation beam with two intensity control reflections measured every 30 min. Lorentz and polarization corrections were applied using the program HELENA (8). The correction for absorption effects ($\mu = 293.1$ cm^{-1}) was calculated with the shape of the crystal as refined against ψ scans by the computer program HABITUS (9). The absorption correction was applied to the data by the program ABSORB (8). The intensity data were averaged in Laue symmetry $2/m$ with an $R_{\text{int}} = 0.005$ resulting in 249 main reflections, 319 satellite reflections of first order, and 324 satellite reflections of second order with $I > 3\sigma(I)$. This data set was used for subsequent structure refinements (Table 1).

3. STRUCTURE DETERMINATION

As a first step the averaged structure was refined against the main reflections ($m = 0$) measured at 15 K. No deviations from $C2/m$ symmetry were observed. Smooth convergence was obtained toward $R_F = 0.0383$ and $wR_F^2 = 0.0479$. As expected for the averaged structure, only minor deviations from the positions of the atoms at room temperature were found. Refinement of the niobium content of this compound did not lead to significant site occupancies for the doping atoms. Therefore niobium was neglected in subsequent refinements. Detailed investigations of the distribution of Niobium atoms in doped $NiTa_2Se_7$ will be published elsewhere (7). All refinements were performed with the program JANA98 (10).

With the second-order satellites included, the symmetry of the modulated state was confirmed to be the superspace group $C2/m(0q_b0)s0$ (5) [the symmetry operators are (x_1, x_2, x_3, x_4), $(-x_1, x_2, -x_3, \frac{1}{2} + x_4)$, $(x_1, -x_2, x_3, \frac{1}{2} - x_4)$, and $(-x_1, -x_2, -x_3, -x_4)$]. The modulation was described by a Fourier series for the modulation functions of each independent atom:

$$u_\alpha^\mu = \sum_{n=1}^{2} A_{n,\alpha}^\mu \sin(2\pi n\bar{x}_4) + B_{n,\alpha}^\mu \cos(2\pi n\bar{x}_4), \qquad [2]$$

$$\bar{x}_4 = \vec{q}\cdot\vec{r} + t. \qquad [3]$$

TABLE 1
Experimental Details

Crystal data	
Chemical formula	$NiTa_{1.98}Nb_{0.02}Se_7$
Chemical formula weight	973.33
Crystal form	Needle
Crystal size (mm)	$0.035 \times 0.05 \times 4$
Crystal color	Black metallic gloss
Cell setting	Monoclinic
Laue symmetry	$2/m$
a(Å)	13.807(6)
b(Å)	3.483(1)
c(Å)	18.564(11)
β(deg)	108.947(40)
Modulation wavevector $\vec{q}$	(0, 0.483(2), 0)
Z	4
D_x (g cm^{-3})	7.24
Radiation type	Synchrotron radiation
Wavelength (Å)	0.5608
No. of reflections for cell parameters	12
θ-range (deg)	12.0–14.0
μ (cm^{-1})	293.1
Data collection	
Experimental station	Beamline D3 Hasylab (Desy Hamburg)
Diffractometer	Huber 4-circle, APD closed-cycle-cryostat
Temperature (K)	15 K
Data collection method	ω scans
Absorption correction	ψ scans + Gaussian integration (Herrendorf 1992)
T_{min}	0.16
T_{max}	0.69
No. of measured reflections	2360
No. of independent reflections	1209
No. of observed reflections	892
Criterion for observed reflections	$I > 3\sigma(I)$
R_{int}	0.005
No. of standard reflections	2
Frequency of standard reflections	Every 30 min
Refinement	
Refinement on	F (using computer program JANA98)
R	0.059
wR	0.053
No. of reflections used	892 (all) 643 (satellite reflections)
No. of parameters used	122 (all) 60 (modulation parameters)
Weighting scheme	$1/\sigma^2(F)$
Extinction method	Isotropic, type 1 (Becker & Coppens, 1974)
Extinction coefficient	0.047
Source of atomic scattering factors	International Tables for Crystallography (1992, Vol. C)

The order of the harmonic is given by n; μ indicates the atom; and $\alpha = x, y, z$. Because satellite reflections up to order 2 were available, Fourier components up to the second harmonic were included into the refinement. All atoms are in mirror planes, on Wyckoff positions $4i$: $(x, 0, z)$. Symmetry restrictions on the modulation functions were derived from the symmetry operator $(x_1, -x_2, x_3, 0.5 - x_4)$, leading to

$$A_{1,y} = B_{1,x} = B_{1,z} = 0, \quad [4]$$

$$A_{2,x} = A_{2,z} = B_{2,y} = 0 \quad [5]$$

for all independent atoms.

Special methods like Patterson methods have not been applied to determine the values of the modulation parameters. Starting from the averaged structure, the first-order harmonics of the modulation functions were introduced. The modulation parameters were refined against the intensities of the main reflections and the first-order satellites for different sets of starting values. Convergence to $R_F = 0.0993$ for the first-order satellites could only be achieved with non-zero starting values for the modulation amplitudes of Ni, Se2, and Se4. All other combinations of starting values lead to a partial R value larger than 0.20.

Subsequently, the second-order harmonics of the modulation functions were introduced. In contrast to the first-order harmonics, a reasonably low R factor for the second-order satellites ($R \approx 0.20$) could only be achieved with predominant values for the second-order harmonics on Ta2, Se1, and Se3. Furthermore the R factor for the first-order satellites was significantly reduced when the second-order harmonics were incorporated on Ta2, Se1, and Se3. This means that the structure model for the second harmonics is in agreement not only with the second-order satellite intensities, but that it also leads to a better fit of the first-order satellites as well even though the contribution of the second harmonic modulation waves to the first order satellite intensities is small.

With all independent parameters free to vary, the refinement converged to final R values of $R_F = 0.0593$ and $wR_F^2 = 0.0531$ (Table 4). Unfortunately the final structure model could not be checked by difference Fourier because of strong series termination effects due to the missing $k = 0$ reflections. This was caused by the restricted area of reciprocal space that could be accessed with the cryostat mounted on the diffractometer.

The parameters of the final structure model are summarized in Tables 2 and 3. It should be noted that the negative temperature parameters U_{11} are not caused by an overestimation of the modulation amplitudes. These negative values already appear in the refinement of the average structure against main reflections only and they are small compared to values of temperature parameters determined at room temperature. They are caused by systematic errors due to the needle shape of the sample, because the length of the sample exceeded the diameter of the beam by a factor of 4. A systematic correction for the changing scattering volume

TABLE 2
Parameters of the Basic Structure of $NiTa_{1.98}Nb_{0.02}Se_7$ after Refinement with Two Harmonics for All Atoms

Atom	x	y	z	U_{11}	U_{22}	U_{33}	U_{13}
Ta1	0.15067(3)	0.0	0.39914(2)	− 0.0089(3)	0.0034(3)	0.0026(3)	− 0.0035(2)
Ta2	0.22905(2)	0.0	0.08986(2)	− 0.0085(3)	0.0051(3)	0.0031(3)	− 0.0027(2)
Ni	0.18927(9)	0.5	0.20890(6)	− 0.0068(7)	0.0048(4)	0.0011(7)	− 0.0030(5)
Se1	0.36646(6)	0.0	0.01299(4)	− 0.0095(5)	0.0019(4)	0.0036(5)	− 0.0045(4)
Se2	0.06115(6)	0.5	0.29486(4)	− 0.0053(6)	0.0036(4)	0.0023(4)	− 0.0063(4)
Se3	0.08074(6)	0.0	0.13693(4)	− 0.0062(5)	0.0026(3)	0.0022(5)	− 0.0034(4)
Se4	0.34644(6)	0.5	0.17386(4)	− 0.0116(5)	0.0038(3)	0.0013(4)	− 0.0056(4)
Se5	0.01887(6)	0.5	0.41832(4)	− 0.0073(6)	0.0042(4)	0.0025(5)	− 0.0021(4)
Se6	0.30108(6)	0.5	0.44660(4)	− 0.0094(5)	0.0020(3)	0.0050(5)	− 0.0034(4)
Se7	0.25881(6)	0.0	0.29996(4)	− 0.0106(5)	0.0039(4)	0.0027(5)	− 0.0052(4)

Note. Given are the fractional coordinates of the atoms, and their temperature parameters U_{ij} in Å^2. Symmetry determines that $U_{12} = U_{23} = 0$. Standard deviations are given in parentheses.

has proven difficult because of the inhomogeneities in the beam profile of the synchrotron radiation. These errors do not affect the accuracy of the structural parameters as can be seen in the excellent fit of the main reflections to the averaged structure, which is in agreement with previous refinements of the average structure (2, 5).

4. DISCUSSION

A model is presented for the incommensurately modulated structure of $NiTa_2Se_7$ in its CDW state. Both the first-order and the second-order harmonics of the modulation functions could be determined. A major feature is that the different harmonics affect different atoms. Maximum modulation amplitudes with the first-order harmonic wave appear predominantly on the Se2 atom and the neighboring Ni atom. The distortion pattern is transverse to the Ni chain. In contrast, the largest distortion with the second-order harmonic can be found on the Ta2 atoms with shifts parallel to the chain directions. All other observed modulation amplitudes can be explained by elastic coupling to the atoms carrying the primary distortions. This is the case in particular for the small distortion amplitudes of the first harmonic found on the Ta2 atoms. They are caused by elastic coupling from the Ni atom via the Se4 atom to the Ta2 atom. A complete picture of the distortion pattern is given in Fig. 1.

The $2q$ component of the modulation cannot be considered as a second-order effect of the q modulation, because both orders affect different parts of the structure. Instead, the q and $2q$ modulations are to be considered as independent modulation waves. Additional support for this interpretation comes from the observed temperature dependence of the diffuse scattering (3). Diffuse intensity related to the q distortion could be observed only below 70 K, while diffuse intensity related to the $2q$ distortion was observed up to 200 K.

The modulation parameters for the first-order harmonics are in excellent agreement with a previous study on pure

TABLE 3
Modulation Amplitudes of All Atoms after the Final Refinement

Atom	$A_{1,x}$	$B_{1,y}$	$A_{1,z}$	$B_{2,x}$	$A_{2,y}$	$B_{2,z}$
Ta1	− 0.0023(6)	0.0281(4)	− 0.0026(6)	0.0016(9)	0.0009(5)	− 0.0022(8)
Ta2	− 0.0258(6)	− 0.0151(4)	− 0.0260(6)	0.0010(11)	− 0.0442(4)	0.0001(11)
Ni	− 0.0552(20)	− 0.0023(12)	0.0481(19)	− 0.0002(28)	0.0011(15)	0.0038(27)
Se1	0.0076(14)	0.0107(9)	0.0069(13)	0.0061(20)	− 0.0087(11)	0.0048(19)
Se2	0.1221(15)	0.0003(10)	− 0.0657(14)	− 0.0019(20)	− 0.0019(11)	0.0035(19)
Se3	− 0.0083(14)	− 0.0241(9)	0.0004(13)	− 0.0044(20)	− 0.0088(11)	0.0017(20)
Se4	− 0.0442(14)	0.0130(9)	0.0279(14)	0.0021(19)	0.0013(11)	0.0064(19)
Se5	0.0205(14)	0.0012(9)	0.0231(13)	− 0.0035(18)	0.0005(11)	− 0.0009(18)
Se6	0.0220(14)	− 0.0006(9)	0.0032(14)	− 0.0003(19)	0.0004(11)	0.0022(19)
Se7	0.0058(14)	− 0.0389(9)	0.0036(14)	0.0008(19)	− 0.0017(11)	− 0.0015(19)

Note. The amplitudes according to Eq. [2] are given in Å along the coordinate axes. The parameters $A_{1,y}$, $B_{1,x}$, $B_{1,z}$, $A_{2,x}$, $A_{2,z}$, and $B_{2,y}$ are equal to zero by symmetry.

TABLE 4
Partial *R* Factors for the Best Structure Model, and the Number of Reflections Used in the Refinements

Reflection group	No. total	No. observed	R_F (%)	wR_F^2 (%)
Main	252	249	3.86	4.80
1-order satellites	464	319	8.83	8.09
2-order satellites	493	324	21.41	23.33
All	1209	892	5.93	5.31

$NiTa_2Se_7$ (5). Furthermore, the transition temperature to the CDW state of the present sample was determined by conductivity measurements as $T_c = 54$ K. This value is close to the transition temperature of the samples used in the previous investigations (3, 5), indicating samples of comparable purity. We expect that the effect of the small amounts of impurities is not responsible for the observed modulation effects, and that the observed pattern of distortions with the second-order harmonic is an intrinsic property of the low-temperature CDW state of $NiTa_2Se_7$.

The pattern of distortions for the $2q$ wave on the chain of Ta2 atoms gives evidence for a regular Peierls distortion with this period. The transverse character of the q modulation on the double chain of Ni and Se2 atoms can only be understood in terms of a CDW under the assumption that the variation of the Ni–Se2 bond valence corresponds to a charge density modulation (5). Alternatively, the two distortions could be related to a CDW and an SDW (spin density wave), respectively. However, indications for a magnetic component of the phase transition have not been found. The most likely explanation for our results is that independent CDWs are present, corresponding to $2k_F$ and $4k_F$ distortions.

Band structure calculations are in favor of this interpretation (11). Overlapping partly filled bands with a low-dimensional character were found on the bicapped trigonal prismatic coordinated Ta1 chain (which includes the Se2 atom) and on the Ta2 chain. With the newly found $2q$ distortions on the Ta2 chain, both low-dimensional electron bands lead to a charge density wave on the related chain. On the other hand, the estimated size of $0.1b^*$ for the Fermi surface nesting vector is not in agreement with the observed modulation wave vector. A $4k_F$ CDW requires a band of strongly correlated electrons. This is not what was found for the subband on the Ta2 atoms (11). At present, a complete understanding of the $2k_F$ and $4k_F$ instabilities observed in $NiTa_2Se_7$ has not yet been achieved.

The results on $NiTa_2Se_7$ can be compared with observations on the organic quasi-one-dimensional conductor TTF-TCNQ (tetrathiafulvalene-tetracyanoquinodimethane). For TTF-TCNQ incommensurate modulations with q' and $2q'$ wave vectors have been found by X-ray diffraction (12). Similar to $NiTa_2Se_7$, the temperature dependence of the diffuse scattering was found to be different for the q' and the $2q'$ scattering. From these observations it was proposed that independent $2k_F$ and $4k_F$ CDW modulations exist in TTF-TCNQ, and these CDWs were related to the different phase transitions observed in this compound. Different models have been proposed to explain the existence of two independent CDWs. The most favorable one is that the $2k_F$ CDW occurs on the TCNQ chain, while the $4k_F$ CDW resides on the TTF chain. The $4k_F$ character of the instability in the TTF chains, then, is caused by strong correlations of the electrons on this chain (13). In contrast to our results on $NiTa_2Se_7$, detailed structural information for TTF-TCNQ is only available for the $2k_F$ modulation (14, 15). The modulation was found to incorporate amplitudes of similar sizes for both the TTF and TCNQ molecules. This contradicts a model of independent CDWs on the independent chains, and the question about the nature of both CDWs in TTF-TCNQ is as yet unresolved.

5. CONCLUSIONS

The modulated low-temperature structure of $NiTa_2Se_7$ was investigated by X-ray diffraction. First- and second-order satellites were measured, so the first- and the second-order harmonics of the modulation functions could be determined. It was found that first-order and second-order harmonics describe different modulation waves in different parts of the structure. The modulation pattern of the first-order harmonics could be confirmed, as it was previously determined by Spijkerman *et al.* (5). The major part of the first-order harmonics is a transverse wave on the Ni and Se2 atoms. The second-order harmonic modulation can be characterized as a longitudinal wave on the Ta2 atoms. With the support of the temperature dependence of the diffuse scattering, it is thus concluded that the q and $2q$ distortions correspond to independent modulation waves.

The most likely explanation for these features is the coexistence of a $2k_F$ CDW and a $4k_F$ CDW, as they can exist on different quasi-one-dimensional electron bands in different parts of the structure.

ACKNOWLEDGMENTS

The authors gratefully acknowledge experimental support by Hans-Georg Krane. We thank E. Riedl for technical assistance in crystal growth. Financial support by the Deutsche Forschungsgemeinschaft under Grant Sm55/3-1 is gratefully acknowledged.

REFERENCES

1. P. Monceau, "Electronic properties of Inorganic Quasi-One-Dimensional Compounds, Part II Experimental" (P. Monceau, Ed.). Reidel, Dordrecht, 1985.
2. S. A. Sunshine and J. A. Ibers, *Inorg. Chem.* **25,** 4355 (1986).

3. R. M. Fleming, S. A. Sunshine, C. H. Chen, L. F. Schneemeyer, and J. V. Waszczak, *Phys. Rev. B* **42,** 4954 (1990).
4. R. E. Peierls, "Quantum Theory of Solids." Clarendon, Oxford, 1975.
5. A. Spijkermann, A. Meetsma, J. L. de Boer, Y. Gao, and S. van Smaalen, *Phys. Rev. B* **52,** 3892 (1995).
6. S. van Smaalen, J. L. De Boer, A. Meetsma, H. Graafsma, H. Sheu, A. Darovskikh, P. Coppens, and E. Levy, *Phys. Rev. B* **45,** 3103 (1992).
7. J. Lüdecke and S. van Smaalen, *Phys. Rev. B* (2000).
8. A. L. Spek and A. Meetsma, HELENA, ABSORB. University of Groningen, The Netherlands, 1981.
9. W. Herrendorf, Ph.D. Thesis. University of Karlsruhe, Germany, 1992.
10. V. Petricek and M. Dusek, Computer code JANA98. Institute of Physics of the Academy of Sciences, Prague, Czech Republic, 1998.
11. E. Canadell and M.-H. Whangbo, *Inorg. Chem.* **26,** 3974 (1987).
12. J. P. Pouget, S. K. Khanna, F. Denoyer, R. Comes, A. F. Garito, and A. J. Heeger, *Phys. Rev. Lett.* **37,** 437 (1976).
13. F. Zwick, D. Jérome, G. Margaritondo, M. Onellion, J. Voit, and M. Grioni, *Phys. Rev. Lett.* **81,** 2974 (1998).
14. P. Coppens, V. Petricek, D. Levendis, K. Finn-Larsen, A. Paturle, G. Yan, and A. D. LeGrand, *Phys. Rev. Lett.* **59,** 1695 (1987).
15. Y. Bouveret and S. Megtert, *J. Phys. France* **50,** 1649 (1989).